ARCHIVES OF ELECTRICAL ENGINEERING VOL. 68(1), pp. 185–194 (2019)

DOI 10.24425/aee.2019.125989

Equation of the magnetic field distribution of dynamo sheets taking into account crystallographic structure

Witold Mazgaj[1], **Zbigniew Szular**[1], **Michał Sierżęga**[1], **Paweł Szczurek**[2]

[1] *Institute of Electromechanical Energy Conversion, Cracow University of Technology*
Warszawska 24, 31-155 Kraków, Poland
e-mails: pemazgaj@cyfronet.pl, {zszular/michal.sierzega}@pk.edu.pl

[2] *Laboratory of magnetic measurements, Stalprodukt SA*
Wygoda 69, 32-700 Bochnia, Poland
e-mail: pawel.szczurek@stalprodukt.pl

(Received: 21.09.2018, revised: 30.11.2018)

Abstract: The main purpose of the paper is to present a method which allows taking into account the anisotropic properties of dynamo steel sheets. An additional aim is to briefly present anisotropic properties of these sheets which are caused by occurrences of some textures. In order to take into account textures occurring in dynamo sheets, a certain sheet sample is divided into elementary segments. Two matrix equations, describing changes of the magnetic field, are transformed to one non-linear algebraic equation in which the field strength components are unknown. In this transformation the flux densities assigned to individual elementary segments are replaced by functions of flux densities of easy magnetization axes of all textures occurring in the given dynamo sheet. The procedure presented in the paper allows determining one non-linear matrix equation of the magnetic field distribution; in this equation all textures occurring in a dynamo sheet are included. Information about textures occurring in typical dynamo sheets may be used in various approaches regarding the inclusion of anisotropic properties of these sheets, but above all, the presented method can be helpful in calculations of the magnetic field distribution in anisotropic dynamo sheets.

Key words: crystallographic texture, dynamo steel sheet, iron crystal, magnetic anisotropy, magnetic field

1. Introduction

Different magnetic measurements carried out using the Epstein frame and Rotational Single Sheet Testers have shown that the majority of the dynamo sheets have certain anisotropic features [1–3]. It has also been confirmed by crystallographic tests carried out on samples of several selected dynamo sheets from different manufacturers [4]. The reason for this is that the iron grains in these sheets create certain textures, i.e. some groups of these grains have privilege crystallographic orientations with respect to the rolling direction of the given dynamo sheet. So, flux densities in particular directions on the dynamo sheet plane change their values in a different way. Anisotropic properties of the dynamo sheets are especially visible comparing hysteresis loops measured along both the rolling and the transverse direction of the given dynamo sheet. Fig. 1 shows the measured hysteresis loops of two different dynamo sheets. Values of the coercive force and of the remanence differ even up to 35 percent with respect to values of these parameters measured for the rolling direction.

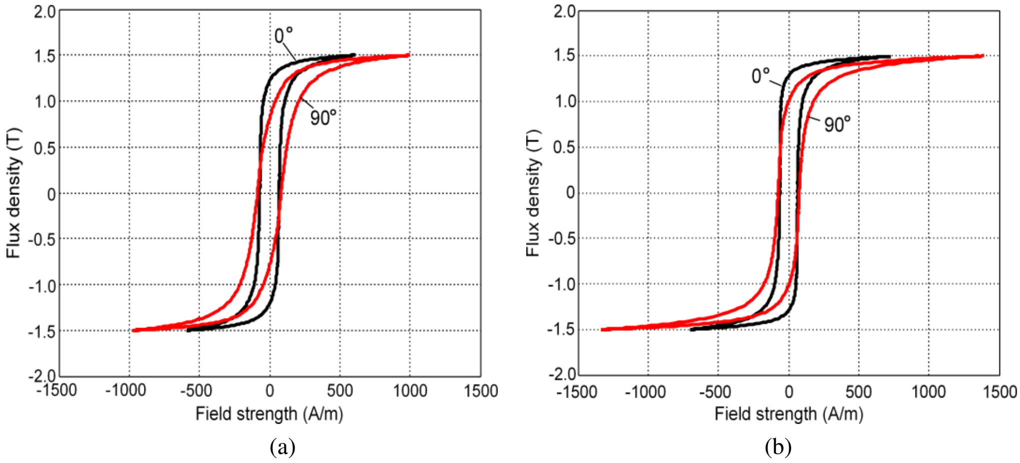

Fig. 1. Hysteresis loops of two different dynamo sheets measured along both the rolling and the transverse directions: M530-50A – South Korea (a); M530-50A – Czech Republic (b)

Several papers present some proposals how to take into considerations the anisotropic properties of dynamo sheets. The so-called elliptical model is widely described in [5] and the model formulated on the co-energy density is discussed in [6–8], however, these models concern non-hysteresis materials. In some studies the magnetic anisotropy of electrical steel sheets has been taken into account using the reluctivity or permeability tensor [9, 10]. The anisotropic properties of dynamo sheets can be relatively easily taken into account in the model of the rotational magnetization which is presented in [11]. In this approach an assumed number of specified directions are determined on the plane of the given dynamo sheet sample, and to each direction a certain hysteresis is assigned, which differs from the hysteresis of the whole anisotropic sheet sample. However, creating this model of the magnetic anisotropy there was assumed that the iron crystals have only one easy magnetization axis. Some researchers have considered the hysteresis modeling of anisotropic materials assuming that these materials have only fiber texture [12] and they suggested to take into consideration different textures occurring in the tested anisotropic materials. Due to the anisotropic properties of the dynamo sheets, the issue of including textures in calculations of a magnetic field is a still valid problem, especially when the magnetization processes have a rotational character.

2. Crystallographic structure of dynamo sheets

Dynamo steel sheets are produced as non-oriented sheets, because these sheets should have isotropic magnetic properties. However, the dynamo sheets can have a significant number of different texture type, unlike transformer sheets where the so-called Goss texture decides about magnetic properties of these sheets. An occurrence of a certain texture means that an amount of iron grains has a privilege crystallographic orientation, usually with respect to the rolling direction, in the given electrical steel sheet; texture types are most often determined using the so-called pole figures [13]. It is understood that including all texture types, which may occur in the tested dynamo sheet, in numerical calculations of a magnetic field is practically impossible. In order to simplify this problem it has been assumed that all textures can be reduced to one of three basic texture types: cube-on-face texture {100}, cube-on-edge texture {110}, and the so-called cube-on-vertex texture {111} (Fig. 2). As magnetic measurements and crystallographic studies have shown, grains of the individual textures are distributed symmetrically with respect to the rolling direction [3, 14]; this is the result of a technological process. Dominant textures of several chosen dynamo sheets, manufactured in different countries, are shown in Table 1; the parameter "Direction angle" denotes the angle between the rolling direction and one of three easy magnetization axes of cubic shaped iron crystals.

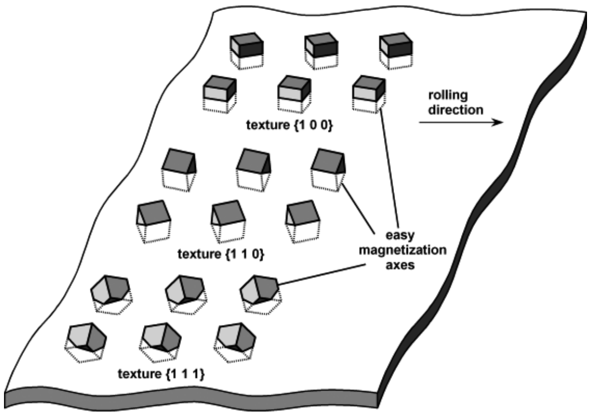

Fig. 2. Examples of the basic textures occurring in dynamo sheets

It is worth underlining that the magnetic properties of the given dynamo sheet depend on both the percentage share of the given texture and on the arrangement of the given texture in the tested dynamo sheet. The percentage share of some textures can be up to over thirty percent with reference to volume of the given dynamo sheet sample.

The influence of the individual texture type on the flux density changes is presented in Fig. 3, which shows hodographs of the flux density for individual textures during rotation of the field strength vector. The flux density hodographs are calculated for some angles between the chosen easy magnetization axis and the rolling direction; it was assumed that in an individual case only one texture type occurs in the tested sheet sample.

Table 1. Dominant types of textures in dynamo sheets

Dynamo sheet	Texture (*)	Share	Direction angle	Dynamo shhet	Texture (*)	Share	Direction angle
M400-50A (Russia)	{100}⟨027⟩	33	16	M530-50A (South Korea)	{100}⟨049⟩	23	24
	{100}⟨057⟩	10	36		{100}⟨011⟩	9	45
	{110}⟨332⟩	29	47		{110}⟨233⟩	34	25
	{111}⟨123⟩	14	30		{111}⟨112⟩	34	0
	{111}⟨145⟩	14	15	M800-50A (Sweden)	{100}⟨049⟩	24	24
M530-50A (Czech Republic)	{100}⟨049⟩	19	24		{100}⟨011⟩	8	45
	{100}⟨011⟩	6	45		{110}⟨111⟩	16	35
	{110}⟨111⟩	25	35		{111}⟨347⟩	41	15
	{111}⟨123⟩	28	30		{111}⟨011⟩	11	0
	{111}⟨112⟩	22	0				

*) For the given texture the parameters u, v, w denote coordinates of the vector which is parallel to the rolling direction; these parameters are determined with respect to the coordinate system of the given texture.

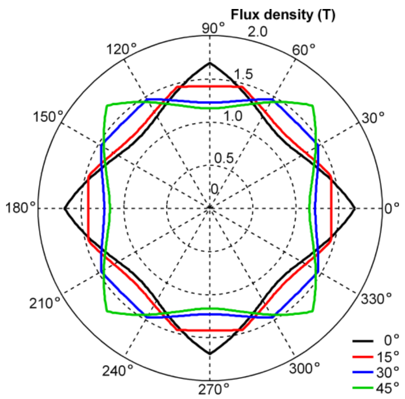

(a)

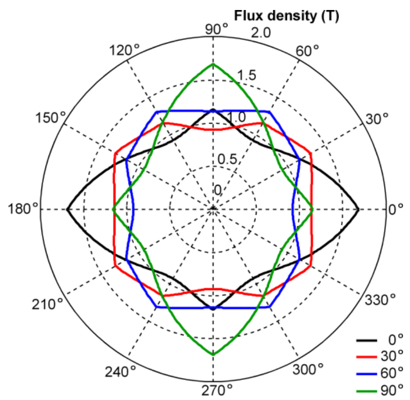

(b)

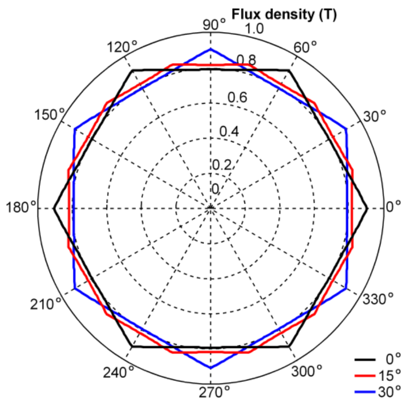

(c)

Fig. 3. Hodographs of the flux density determined for individual textures: cube-on-face texture {100} (a); cube-on-edge texture {110} (b); cube-on-face vertex {111} (c)

3. Basic equations of the magnetic field distribution

In order to formulate equations of the magnetic field distribution, a sample of the given dynamo sheet is divided into elementary segments which have the same crystallographic structure. Each field strength component is assigned to only one branch of the division grid consisting of edges of the elementary segments (Fig. 4(a)). Due to non-linear and anisotropic properties of the dynamo sheets, each elementary segment has to be divided into four subsegments, because the field strength and the flux density change their values in the given subsegment differently to other subsegments. So, the components of the flux density are assigned as it is shown in Fig. 4(b); it was assumed that the magnetic field in dynamo sheets has two-dimensional character. The flux density components that are assigned to the left bottom and right upper subsegments should be taken into account in order to unambiguously determine the magnetic field distribution.

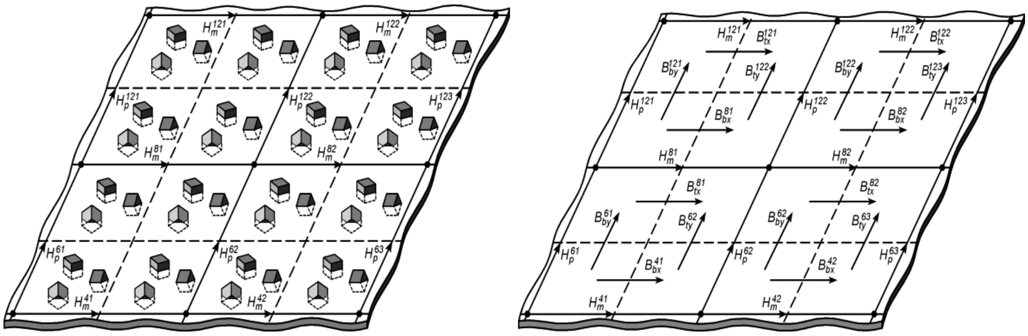

(a) (b)

Fig. 4. Division of a sheet sample on elementary segments and subsegments (a), example of description of the field strength and flux density components (b); superscripts denote the consecutive numbers of the components

On the basis of Maxwell's equations in their integral form, relating to the magnetic field, the matrix equations describing the distribution of the magnetic field can be formulated; it is widely described in [15]. These equations have the following matrix form:

$$\boldsymbol{A_m H_m} + \boldsymbol{A_p H_p} = \boldsymbol{S_J J_{ex}}\,, \tag{1}$$

$$\boldsymbol{C_{bx} B_{bx}} + \boldsymbol{C_{by} B_{by}} + \boldsymbol{C_{ux} B_{ux}} + \boldsymbol{C_{uy} B_{uy}} = 0, \tag{2}$$

where: $\boldsymbol{H_m}$, $\boldsymbol{H_p}$ are the column vectors of the field strength components H_m, H_p; $\boldsymbol{A_m}$, $\boldsymbol{A_p}$ are the matrixes of distances between vertexes of the division grid, $\boldsymbol{S_J}$ denotes the matrix of surfaces of the meshes related to division of the sheet sample, $\boldsymbol{J_{ex}}$ is the column vector of the current density values of the external currents, $\boldsymbol{B_{bx}}$, $\boldsymbol{B_{by}}$, $\boldsymbol{B_{ux}}$, $\boldsymbol{B_{uy}}$ are the column vectors of flux density components B_{bx}, B_{by}, B_{ux}, B_{uy}, $\boldsymbol{C_{bx}}$, $\boldsymbol{C_{by}}$, $\boldsymbol{C_{ux}}$, $\boldsymbol{C_{uy}}$ denote the matrixes of segment face areas which are penetrated by magnetic fluxes with the corresponding components; $\boldsymbol{A_m}$, $\boldsymbol{C_{ux}}$, $\boldsymbol{C_{uy}}$ are the square matrixes.

Magnetization processes are caused by changes of the field strength in particular segments [16], so these two equations have to be transformed into one matrix equation in which the column vector $\boldsymbol{H_p}$ is unknown. The flux density components should be written as appropriate functions of the corresponding components of the field strengths H_m, H_p. When the magnetization processes are related to movements of domain walls then these processes should be considered along the easy magnetization axes of the iron grains of the individual textures occurring in the tested dynamo sheet.

4. Changes of the flux density along easy magnetization axes

In order to take into account textures, values of the field strengths of all the easy magnetization axes should be saved as functions of the field strength components that are associated with the branches of the elementary segments (Fig. 4). As previously mentioned, each texture is distributed symmetrically with respect to the rolling direction (Fig. 2), therefore the field strengths should be determined for the three axes of easy magnetization of both parts of individual textures. For the first part of the cube-on-face texture {100} (Fig. 5(a)) of the bottom subsegments it can be written as follows:

$$\boldsymbol{H_{fb1a}} = f_{hf1am}\,\boldsymbol{M_{bm}}\,\boldsymbol{H_m} + f_{hf1ap}\,\boldsymbol{M_{bp}}\,\boldsymbol{H_p}\,, \tag{3a}$$

$$\boldsymbol{H_{fb2a}} = f_{hf2am}\,\boldsymbol{M_{bm}}\,\boldsymbol{H_m} + f_{hf2ap}\,\boldsymbol{M_{bp}}\,\boldsymbol{H_p}\,, \tag{3b}$$

and for the second part of this texture:

$$\boldsymbol{H_{fb1b}} = f_{hf1bm}\,\boldsymbol{M_{bm}}\,\boldsymbol{H_m} + f_{hf1bp}\,\boldsymbol{M_{bp}}\,\boldsymbol{H_p}\,, \tag{3c}$$

$$\boldsymbol{H_{fb2b}} = f_{hf2bm}\,\boldsymbol{M_{bm}}\,\boldsymbol{H_m} + f_{hf2bp}\,\boldsymbol{M_{bp}}\,\boldsymbol{H_p}\,, \tag{3d}$$

where: $\boldsymbol{H_{fb1,2a,b}}$ are the column vectors of the field strength values of the easy magnetization axes ($\boldsymbol{f}$, f represent the cube-on-face texture, $\boldsymbol{b}$, b represent the bottom subsegments, 1, 2 are the first, and second easy magnetization axes, respectively, $\boldsymbol{a}$, a, $\boldsymbol{b}$, b are the parts of the considered texture symmetrically distributed with respect to the rolling direction), $\boldsymbol{M_{bm}}$, $\boldsymbol{M_{bp}}$ are the matrixes that assign field strength components of the easy magnetization axes to the appropriate components H_m, H_p, $f_{hf\,1,2\,a,mp}$ are the appropriate trigonometric relationships that allows us to save the field strength of easy magnetization axes as functions of the field strength components of the division grid. Please notice that the third easy magnetization axis of the iron crystals is perpendicular to the sheet plane, so the field strength of this axis is equal to zero.

Relationships determining the field strengths of the easy magnetization axes of the cube-on-edge texture {110} as functions of the field strength components H_m, H_p have a similar form as previous relations, because considering this texture, changes of the magnetic field strength along the second and third easy magnetization axis are the same (Fig. 5(c)). In order to take into account the influence of the cube-on-vertex texture {111} on magnetization processes, the field strengths for all the easy magnetization axes of this texture should be saved separately. For the first part of the cube-on-vertex texture {111} of the bottom subsegments it can be saved as (Fig. 5(c)):

$$\boldsymbol{H_{vb1a}} = f_{hv1am}\,\boldsymbol{M_{bm}}\,\boldsymbol{H_m} + f_{hv1ap}\,\boldsymbol{M_{bp}}\,\boldsymbol{H_p}\,, \tag{4a}$$

$$\boldsymbol{H_{vb2a}} = f_{hv2am}\,\boldsymbol{M_{bm}}\,\boldsymbol{H_m} + f_{hv2ap}\,\boldsymbol{M_{bp}}\,\boldsymbol{H_p}\,, \tag{4b}$$

$$\boldsymbol{H_{vb3a}} = f_{hv3am}\,\boldsymbol{M_{bm}}\,\boldsymbol{H_m} + f_{hv3ap}\,\boldsymbol{M_{bp}}\,\boldsymbol{H_p}\,, \tag{4c}$$

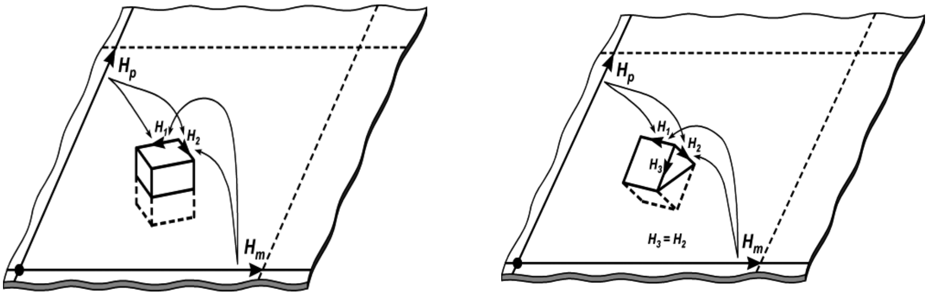

(a) (b)

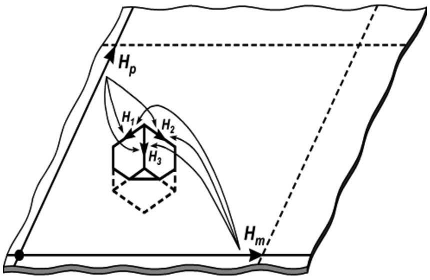

(c)

Fig. 5. Determination of the field strength in easy magnetization axes as dependences on the field strength components H_m, H_p; cube-on-face texture $\{100\}$ (a); cube-on-edge texture $\{110\}$ (b); cube-on-face vertex $\{111\}$ (c)

and for the second part of this texture:

$$\boldsymbol{H_{vb1b}} = f_{hv1bm}\, \boldsymbol{M_{bm}}\, \boldsymbol{H_m} + f_{hv1bp}\, \boldsymbol{M_{bp}}\, \boldsymbol{H_p}\,, \tag{4d}$$

$$\boldsymbol{H_{vb2b}} = f_{hv2bm}\, \boldsymbol{M_{bm}}\, \boldsymbol{H_m} + f_{hv2bp}\, \boldsymbol{M_{bp}}\, \boldsymbol{H_p}\,, \tag{4e}$$

$$\boldsymbol{H_{vb3b}} = f_{hv3bm}\, \boldsymbol{M_{bm}}\, \boldsymbol{H_m} + f_{hv3bp}\, \boldsymbol{M_{bp}}\, \boldsymbol{H_p}\,, \tag{4f}$$

where $\boldsymbol{v}$, v denote the cube-on-vertex texture $\{111\}$. The matrixes $\boldsymbol{M_{bm}}$, $\boldsymbol{M_{bp}}$ have the same form in each relationship because they determine which components of the field strengths H_m, H_p refer to the individual subsegments. A similar form have relationships concerning the upper right subsegments. The number of elements of the column vector containing field strengths of the easy magnetization axes is equal to the number of elementary segments.

In the next step, flux densities b_a of the easy magnetization axes of all textures should be written as non-linear functions of the field strengths of these axes in the form:

$$b_a = b_{a\,sat}\, f_n(h_a), \tag{5}$$

where: $b_{a\,sat}$ denotes the saturation flux density of the given axis of the easy magnetization (edges of the cubic), $f_n(h_a)$ is a non-linear function of the field strength h_a of this axis; field strengths h_a are dependent on the field strength components H_m, H_p.

The saturation flux density $b_{a\,sat}$ associated with the given easy magnetization axis of the considered texture is directly proportional to the percentage share of this texture with respect to the whole volume of the given sheet sample. However, it should be strongly emphasized that saturation flux densities of individual axes of easy magnetization do not have a constant value unlike approaches which have assumed that iron crystals have only one axis of the easy magnetization. In a general case, the saturation flux densities $b_{a\,sat}$ are the functions of the angle between the chosen easy magnetization axis and the direction of the field strength occurring on the given subsegment; this problem is widely described in [4]. The relationships in form (5) for the individual easy magnetization axis of all subsegments can be written using appropriate column vectors, e.g. considering easy magnetization axes 2 of the cube-on-face texture {100} for the left bottom subsegment it can be saved as:

$$\boldsymbol{B_{fb2a}} = \boldsymbol{B_{fb\,sat\,2a}} * \boldsymbol{F_n}(\boldsymbol{H_{fb\,2a}}), \tag{6}$$

where: $\boldsymbol{B_{fb\,sat\,2a}}$ is the column vector of the saturation flux densities $b_{fb\,sat\,2a}$ referring to the given easy magnetization axis, "*" denotes the multiplication of two column vectors.

For all the easy magnetization axes of all textures in the bottom and upper subsegments the last relationship can be written as follows:

$$\boldsymbol{B_{tb1,2,3\,a,b}} = \boldsymbol{B_{tb\,sat1,2,3\,a,b}} * \boldsymbol{F_n}(\boldsymbol{H_{tb\,1,2,3\,a,b}}), \tag{7a}$$

$$\boldsymbol{B_{tu1,2,3\,a,b}} = \boldsymbol{B_{tu\,sat1,2,3\,a,b}} * \boldsymbol{F_n}(\boldsymbol{H_{tu\,1,2,3\,a,b}}), \tag{7b}$$

where: $\boldsymbol{t}$ denotes the type of texture, $\boldsymbol{b}$, $\boldsymbol{u}$ refer to the left bottom subsegment and right upper subsegment, respectively. The flux densities in easy magnetization axes are dependent on the field strength component H_m, H_p, because column vectors $\boldsymbol{H_{tb\,1,2,3a,\,b}}$, $\boldsymbol{H_{tu\,1,2,3a,\,b}}$ are determined as functions of the vectors $\boldsymbol{H_m}$, $\boldsymbol{H_p}$.

5. Equations of the magnetic field

Remembering that column vectors $\boldsymbol{B_{bx}}$, $\boldsymbol{B_{by}}$, $\boldsymbol{B_{ux}}$, $\boldsymbol{B_{uy}}$ in Eq. (2) should be replaced by appropriate functions of the vectors $\boldsymbol{H_m}$, $\boldsymbol{H_p}$, the flux densities of the individual easy magnetization axes of all textures are projected onto the sheet plane and then the components B_{bx}, B_{by}, B_{ux}, B_{uy} of the corresponding column vectors occurring in Eq. (2) are determined (Fig. 6). These components are nonlinear functions of the field strength components H_m, H_p. Assuming that in the tested dynamo sheet only there basic textures occur, the column vector $\boldsymbol{B_{bx}}$ can be saved as follows:

$$\begin{aligned}\boldsymbol{B_{bx}} = {} & f_{bxf1a}\boldsymbol{M_{bx}B_{fb\,1a}} + f_{bxf1b}\boldsymbol{M_{bx}B_{fb\,1b}} + f_{bxf2a}\boldsymbol{M_{bx}B_{fb\,2a}} + f_{bxf2b}\boldsymbol{M_{bx}B_{fb\,2b}} + \\ & + f_{bxe1a}\boldsymbol{M_{bx}B_{eb\,1a}} + f_{bxe1b}\boldsymbol{M_{bx}B_{eb\,1b}} + 2f_{bxe2a}\boldsymbol{M_{bx}B_{eb\,2a}} + 2f_{bxe2b}\boldsymbol{M_{bx}B_{eb\,2b}} + \\ & + f_{bxv1a}\boldsymbol{M_{bx}B_{vb\,1a}} + f_{bxv1b}\boldsymbol{M_{bx}B_{vb\,1b}} + f_{bxv2a}\boldsymbol{M_{bx}B_{vb\,2a}} + f_{bxv2b}\boldsymbol{M_{bx}B_{vb\,2b}} + \\ & + f_{bxv3a}\boldsymbol{M_{bx}B_{vb\,3a}} + f_{bxv3b}\boldsymbol{M_{bx}B_{vb\,3b}},\end{aligned} \tag{8}$$

where: functions type $f_{bxf,e,v1,2,3a,b}$ are the trigonometric dependences which allow us to determine the projections of the flux densities in easy magnetization axes on the flux density components B_{bx} of the left bottom subsegments of the dynamo sheet. The first line of the last equation concerns two easy magnetization axes of the cube-on-face texture; in this case the third axis of iron crystals is perpendicular to the sheet plane. A similar case applies to the cube-on-edge texture, because changes of the flux density with respect to axis 2 and 3 are the same. It is necessary to stress that quite often two textures of the same type occur in a given dynamo sheet; the difference between them is related to the angle between chosen easy magnetization axis and the rolling direction.

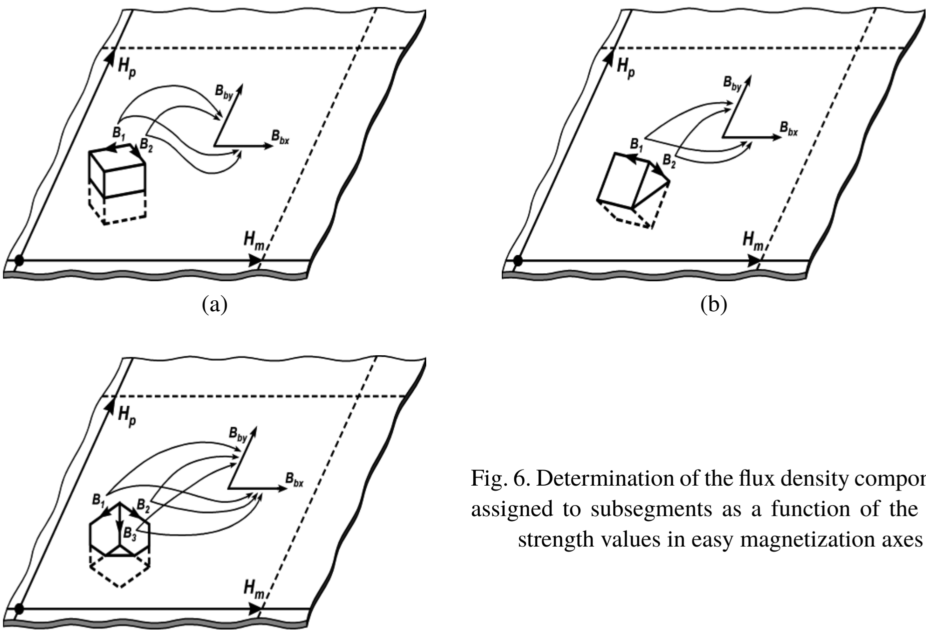

(a) (b) (c)

Fig. 6. Determination of the flux density components assigned to subsegments as a function of the field strength values in easy magnetization axes

The column vectors $\boldsymbol{B_{by}}, \boldsymbol{B_{ux}}, \boldsymbol{B_{uy}}$ have the similar form as $\boldsymbol{B_{bx}}$, and they depend on the vectors $\boldsymbol{H_m}, \boldsymbol{H_p}$. The vector $\boldsymbol{H_m}$, can be eliminated using (1), so (2) can be transformed to the form which contains only the column vector $\boldsymbol{H_p}$. The final nonlinear matrix equation can be solved using the Newton–Raphson method for the assumed values of the current inducing the magnetic field. It is well known that the changes of the magnetic field depend on the eddy currents occurring in the dynamo sheets and vice versa. In this case a separate division grid for the eddy currents should be created and these grids should be connected with each other.

6. Conclusions

The anisotropic properties of the dynamo sheets are the result of the occurrence of some textures in these sheets. These properties depend on both the texture type and the percentage share of the given texture with respect to the whole volume of the dynamo sheet sample. In order to take into account these properties, changes of the flux density along each easy magnetization axis of all textures should be included in the equations determining the magnetic field distribution in the dynamo sheet sample.

This paper proposes the method how to formulate one matrix non-linear equation that allows one to calculate the magnetic field distribution in a given dynamo sheet. In this purpose, the flux densities of easy magnetization axes of all textures are saved as functions of the field strength components which are assigned to branches of the division grid. These flux densities are projected on the sheet plane, and as a result the flux density components which are assigned to the elementary subsegments can be written as an appropriate function of the field strength components that are assigned to branches of the division grid. The validation of the correctness of the magnetic field equation requires consideration of eddy currents which, in turn, influence the magnetic field distribution in electric steel sheets.

Acknowledgements

The research presented in this paper was funded by subsidies granted by Polish Ministry of Science and Higher Education under the theme no. E-2/650/2017/DS – *Modeling of magnetization processes in magnetic circuits of electrical machines and devices for diagnostics and loss estimation*.

References

[1] Soiński M., Moses A.J., *Handbook of magnetic material*, Elsevier Science B.V. (1994).

[2] Tumański S., *Handbook of magnetic measurements*, CRC/Taylor & Francis (2011).

[3] Mazgaj W., Warzecha A., *Influence of electrical steel sheet textures on their magnetization curves*, Archives of Electrical Engineering, vol. 62 (245), no. 3, pp. 425–437 (2013).

[4] Banach A., Mazgaj W., Szular Z., Szczurek P., Zelechowski J., *Textures of dynamo steel sheets*, 2017 International Symposium on Electrical Machines (SME), Naleczow, Poland (2017).

[5] Dedulle J.M., Meunier G., Foggia A., Sabonnadiere J.C., *Magnetic fields in nonlinear anisotropic grain-oriented iron-sheet*, IEEE Transactions on Magnetics, vol. 26, no. 2, pp. 524–527 (1990).

[6] Mekhiche M., Péra T., Maréchal Y., *Model of the anisotropy behaviour of doubly oriented and non-oriented materials using coenergy: application to a large generator*, IEEE Transactions on Magnetics, vol. 31, no. 3, pp. 1817–1820 (1995).

[7] Dupre L.P., van Keer R., Melkeebeek J.A., *Numerical evaluation of the influence of anisotropy on the eddy currents in laminated ferromagnetic alloys*, IEEE Transactions on Magnetics, vol. 38 no. 2, pp. 813–816 (2002).

[8] Lin D., Zhou P., Badics Z., Fu W.N., Chen Q.M., Cendes Z.J., *A new nonlinear anisotropic model for soft magnetic materials*, IEEE Transactions on Magnetics, vol. 42, no. 4, pp. 963–966 (2006).

[9] Enokizono M., Mori S., *A treatment of the magnetic reluctivity tensor for rotating magnetic field*, IEEE Transactions on Magnetics, vol. 33, no. 2, pp. 1608-1611 (1997).

[10] Sande H.V., Boonen T., Podoleanu I., Henrotte F., Hameyer K., *Simulation of a three-phase transformer using an improved anisotropy model*, IEEE Transactions on Magnetics, vol. 40, no. 2, pp. 850–855 (2004).

[11] Mazgaj W., *Modelling of rotational magnetization in anisotropic sheets*, COMPEL, vol. 30, no. 3, pp. 957–967 (2011).

[12] Shi Y.M., Jiles D.C., Ramesh A., *Generalization of hysteresis modelling to anisotropic and textured materials*, Journal of Magnetism and Magnetic Materials, vol. 187, iss. 1, pp. 75–78 (1998).

[13] Bunge H.J., *Texture analysis in materials science: Mathematical methods*, Butterworth (1982).

[14] Wohlfarth E.P., *Ferromagnetic materials. A handbook on the properties of magnetically ordered substances*, North-Holland Publishing Company (1980).

[15] Warzecha A., Mazgaj W., *Magnetization measurements in circle-shaped samples of typical dynamo steel sheets*, Przegląd Elektrotechniczny, no. 6, pp. 96–99 (2015).

[16] Della Torre E., *Magnetic hysteresis*, IEEE Press (1999).